Journal of Applied Polymer Science

Synthesis and Swelling Behaviors of Semi-IPNs Superabsorbent Resin Based on Chicken Feather Protein

Qian Li,[1] Jia Liu,[1] Yuan Su,[1,2] Qinyan Yue,[1] Baoyu Gao[1]

[1]Shandong Key Laboratory of Water Pollution Control and Resource Reuse, School of Environmental Science and Engineering, Shandong University 250100 Jinan, People's Republic of China

[2]School of Mathematic and Quantitative Economics, Shandong University of Finance and Economics, 250100 Jinan, People's Republic of China

Correspondence to: Q. Li (E-mail: qianli@sdu.edu.cn)

ABSTRACT: A novel chicken feather protein-*g*-poly (potassium acrylate)/polyvinyl alcohol (CFP-*g*-PKA/PVA) semi-IPNs superabsorbent resin (SAR) based on feather protein, acrylic acid (AA), and polyvinyl alcohol (PVA) was synthesized by graft copolymerization and semi-interpenetrating technology. The results from FTIR, SEM, and TGA analysis showed that both CFP and PVA reacted with PKA during the polymerization process. The effects of AA, PVA, initiator and crosslinker content on water absorbency of semi-IPNs SAR were studied. The swelling behavior in various pHs and saline solutions were also investigated. The water absorbency of SAR reached the maximum at pH = 6. The effect of the five cations on swelling had the following order: $Al^{3+} > Ca^{2+} > Mg^{2+} > K^{+} > Na^{+}$. The highest water absorbency in distilled water and 0.9 wt % NaCl solutions were 714.22 and 70.08 g g^{-1}, respectively. © 2013 Wiley Periodicals, Inc. J. Appl. Polym. Sci. **2014**, *131*, 39748.

KEYWORDS: grafting; resins; swelling

Received 27 March 2013; accepted 9 July 2013
DOI: 10.1002/app.39748

INTRODUCTION

Superabsorbents are hydrophilic three-dimensional polymeric networks that can absorb, swell and retain a large volume of water or other biological fluids.[1] Because of the superior properties, superabsorbent resin (SAR) enhances its applications in biomedical fields and in industries such as actuators, drug delivery, artificial muscles, sensors, and different chemomechanical devices.[2] Semi-interpenetrating polymer networks (semi-IPNs) are characterized by the penetration on a molecular scale of networks by some of the linear or branched macromolecules.[3] The additional noncovalent interaction between two polymers would influence the morphology and thermal properties of the semi-IPN gel.[4] Semi-IPNs SAR exhibited changes in their swelling and deswelling ratio in response to external stimuli, such as temperature, pH, and ionic concentration.[5] Recently, the use of natural materials such as cellulose,[6] starch,[7] and chitosan[8] for SARs, especially for semi-IPNs SARs applications has attracted more attentions due to their high swelling capacity, low cost, nontoxic, and biodegradability characteristics.

Feathers are composed of over 90% hard to degrade beta-keratin, a fibrous and insoluble protein highly cross-linked with disulfide and other bonds.[9] The complexity of keratin structure is due to the high crosslinking between the polypeptide chains as a result of S—S bonds, hydrogen bonds, and hydrophobic interactions.[10] Feathers have been used in agriculture production as an animal protein supplement[11] or as slow-releasing nitrogen fertilizer.[12] However, the effective use of feather has been limited because that keratin is insoluble and it's hard to be digested by enzyme. In the past few years, several pretreatment methods, including chemical, enzymatic or biological treatments, have been therefore investigated to improve the digestibility of feathers.[13,14]

In fact, protein, which is a kind of hydrophilic material, contains many hydrophilic groups, such as carboxyl, amino, hydroxyl, and sulfydryl can easily actuate a series of chemical reactions. Meanwhile, polyvinyl alcohol (PVA) is widely used as hydrophilic biopolymer in controlled release drug delivery system because of its strength, pH, as well as temperature stability and semicrystalline nature.[15] So far, there is few similar article or relevant study on feather protein-based SAR, especially information concerning the semi-IPNs SAR prepared from chicken feather protein (CFP). Compared with hair keratin protein SAR[16] and soy protein porous SAR,[17] CFP semi-IPNs SAR has better bioadhesive property, biodegradability, and chemical resistance. So in the present article, it is expected to provide a

new method for the utilization of discarded chicken feather and synthetization of semi-IPNs SAR by introducing CFP and PVA.

The present work described the preparation of a novel chicken feather protein-g-poly (potassium acrylate)/polyvinyl alcohol (CFP-g-PKA/PVA) semi-IPNs superabsorbent resin (SAR), which was synthesized in aqueous solutions by a graft copolymerization method using CFP as a basic macromolecular skeletal material, acrylic acid (AA) as a monomer, and PVA as a polymer. The structure, morphology, and thermal stability of SARs were characterized by Fourier transformation infrared spectra (FTIR), scanning electron microscope (SEM), and thermogravimetric analysis (TGA). Meanwhile, the effects of pH and saline solutions on the performance of semi-IPNs SAR in absorbing water were also investigated. The introduction of feather protein in the preparation of SAR, on one hand, can explore a new field of application of discarded feathers; on the other hand, can reduce production cost and improve biodegradability of SAR to a certain extent. Also the presence of PVA as a polymer can enhance the mechanical stability and water absorbency properties through semi-interpenetrating technology.

EXPERIMENTAL

Materials

Acrylic acid (AA), potassium persulfate ($K_2S_2O_8$), ammonium cerium nitrate ($(NH_4)_2Ce(NO_3)_6$), sodium sulfite (Na_2SO_3), *N*,*N*′-methylenebisacrylamide (MBA), potassium hydroxide (KOH) and polyvinyl alcohol (PVA) with the molecular weight of 1.8 hundred thousand were all of analytical grade. Distilled water was used for polymerization and swelling experiments. The concentration of initiators and MBA were 2.0 g/100 mL dist. water.

Pretreatment of Chicken Feather

The chicken feathers were washed and dried in a drying oven at 70°C. A grinder was used to crush chicken feathers, which made feathers pulverized and milled through 10- to 20-mesh screen. The 14 g dried chicken feathers which contained 80% keratin were dipped in 400 mL 0.45% KOH solution, and heated at 90°C for 1.5 h. Finally, the mixture was filtered to remove insoluble substances and 250 mL feather protein extracts were obtained. Sweden Foss-2300 automatic kjeldahl apparatus was used to measure the nitrogen content, and the mass concentration of feather protein was 24 mg mL^{-1}. It can be calculated that 53.6% CFP were obtained. The main chemical makeup of CFP is cystine, and cysteine amino acid residues are most common. Meanwhile, the molecular weight of CFP is mainly distributed between 25,000 and 35,000.

Synthesis of CFP-g-PKA/PVA Semi-IPNs SAR

A series of CFP-*g*-PKA/PVA semi-IPNs SARs with different amounts of PKA, PVA and crosslinker were prepared according to the following procedure. The water bath was heated slowly to 50°C and maintained at this temperature during the whole process. Feather protein extracts, $K_2S_2O_8$ and $(NH_4)_2Ce(NO_3)_6$ were simultaneously put in a 250-mL three-necked flask equipped with a stirrer. After 15 min, AA with 75% neutralization degree (neutralized with 60 mg L^{-1} KOH) and Na_2SO_3 were gradually added into the above solution. Then PVA was

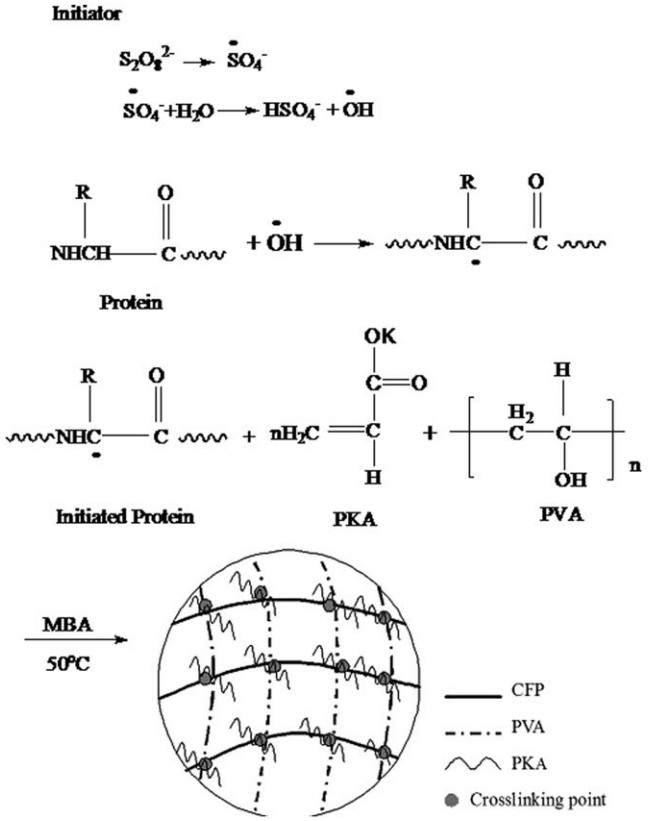

Figure 1. Scheme of graft-copolymerization of CFP-*g*-PKA/PVA semi-IPNs SAR.

added after 15 min polymerization reaction between CFP and AA. After 45 min, appropriate amount of MBA was charged into the flask. Finally the mixture was stirred for 4 h and the resulting products were dried at 70°C to a constant weight. The scheme of graft-copolymerization of CFP-*g*-PKA/PVA semi-IPNs SAR was depicted in Figure 1. The procedure of preparation of chicken feather protein-g-poly (potassium acrylate) superabsorbent resin (CFP-*g*-PKA SAR) and potassium acrylate/polyvinyl alcohol superabsorbent resin (PKA/PVA SAR) were similar to that of CFP-*g*-PKA/PVA semi-IPNs SAR, except without addition of CFP and PVA, respectively. All samples were milled through a 20- to 40-mesh screen.

Characterization

The spectroscopic analyses of samples were characterized by a Fourier transform infrared spectrometer (Thermo nicolet, NEXUS −470) in the range of 4000–400 cm^{-1} using KBr pellet. The samples were gold-coated in a Hitachi S-520 scanning electron microscope (Tokyo, Japan) to analyze the internal morphologies. Thermogravimetric Analysis (TGA) was carried out in a nitrogen atmosphere with the temperature range from 10 to 600°C. The samples were performed with a 10°C min^{-1} heating rate.

Measurement of Swelling Behavior

In the experiment, 0.20 g sample was immersed in excess distilled water and kept undisturbed to reach swelling equilibrium. Then swollen samples were filtered through a 100-mesh gauze

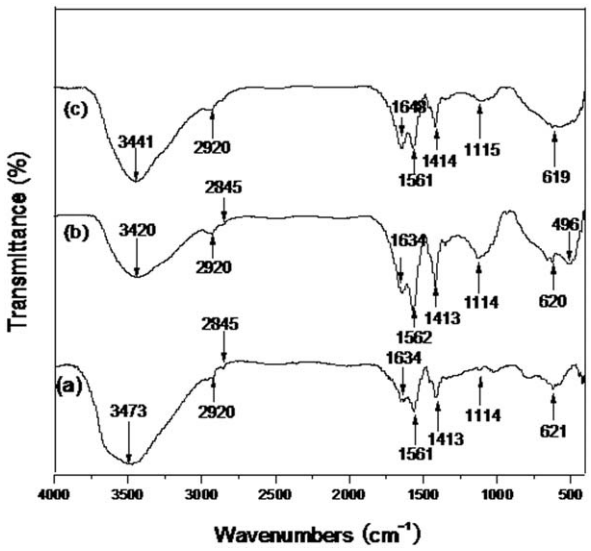

Figure 2. FTIR spectra of CFP-g-PKA SAR (a), PKA/PVA SAR (b) and CFP-*g*-PKA/PVA semi-IPNs SAR (c).

to separate from unabsorbed water and weighted. The water absorption amount Q_{eq} (g/g) was calculated as follows:

$$Q_{eq} = (M_2 - M_1)/M_1 \quad (1)$$

where M_1 (g) and M_2 (g) are the weights of the dry and swollen sample, respectively. Q_{eq} was calculated as grams of water per gram of sample. Water absorbency of samples in both distilled water and 0.9 wt % NaCl solutions were tested in the same way.

Measurement of Swelling Kinetics in Solutions of Various pHs and Saline Ions

Swelling kinetics of SARs in distilled water was measured as follows: an accurate amount of samples (0.20 g) were contacted with distilled water in 500-mL Erlenmeyer flask. The swollen SARs were filtered using a 100-mesh gauze at different intervals. After weighing, the swelling capacity of SARs at a certain moment was calculated according to eq. (1). All samples were carried out three times repeatedly and the averages were reported in this article.

To study the swelling behaviors of semi-IPNs SAR in solutions with different pHs, various pH solutions were adjusted using 1 mol L^{-1} NaOH and 1 mol L^{-1} HCl aqueous solutions. To investigate the effect of different ions on the swelling property of semi-IPNs SAR, various saline solutions (NaCl, KCl, $MgCl_2$, $CaCl_2$, $AlCl_3$ and Na_2SO_4) with 10 mmol L^{-1} were used.

RESULTS AND DISCUSSION

FTIR Results

FTIR was carried out to characterize the chemical structure differences among CFP-g-PKA SAR (a), PKA/PVA SAR (b) and CFP-g-PKA/PVA semi-IPNs SAR (c). The FTIR spectrums of them were shown in Figure 2. As can be seen, the three FTIR spectrums showed same absorption peaks at 2920 cm^{-1} (CH_2-assymetric stretching), 1562 cm^{-1} (—COO^- stretching vibration), 1413 cm^{-1} (C—O—C stretching), 1114 cm^{-1} (υC=O of acrylic acid) and 620 cm^{-1} for hydroxyl groups.

FTIR spectra showed that the characteristic spectra peaks of the samples had some changes, which suggested that the serial compositions of SAR had changed during the polymerization.[8] Compared with absorption peaks of CFP-*g*-PKA/PVA semi-IPNs SAR [Figure 2(c)], the absorption bands at 3473 cm^{-1} (a) and 3420 cm^{-1} (b) for N—H bending of peptide bonds (—CONH—) shifted to 3441 cm^{-1}, which indicated the crosslinking reaction and more disordering structure of semi-IPNs SAR. And, absorption peaks at 1634 cm^{-1} [Figure 2(a,b)] for C=O of amide=band shifted to 1648 cm^{-1} [Figure 2(c)] also provided the evidence. The disappeared absorption bands at 2845 cm^{-1} (CH_2-symmetric stretching) and 496 cm^{-1} indicated that the graft copolymerization and crosslinking process between hydroxyl groups on CFP, PVA, and AA occurred during

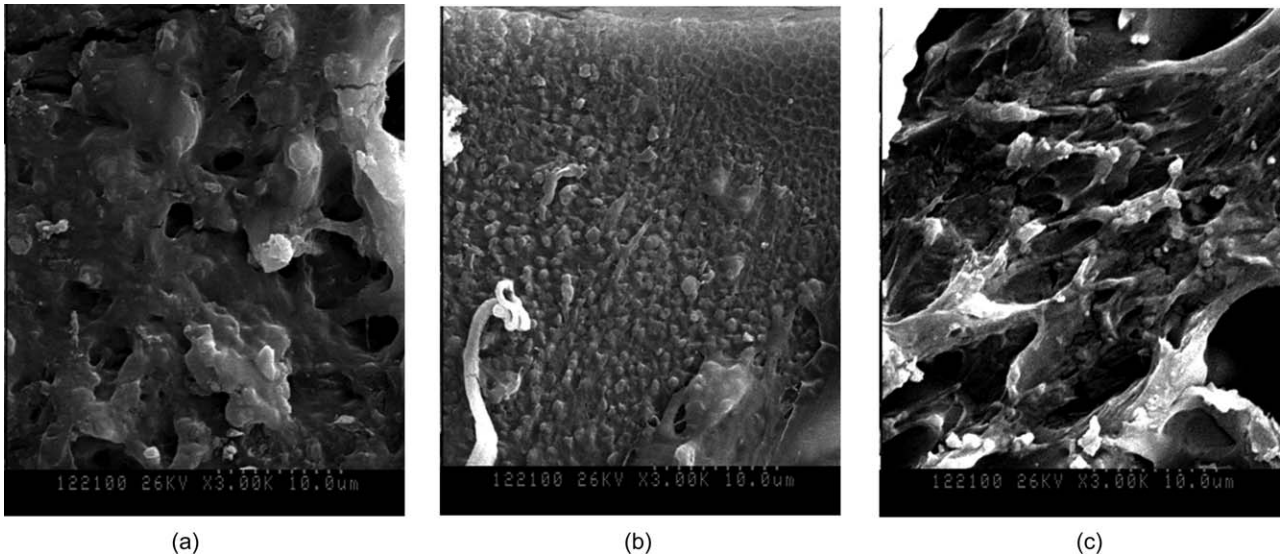

Figure 3. SEM micrographs of CFP-*g*-PKA SAR (a) and PKA/PVA SAR (b) and CFP-*g*-PKA/PVA semi-IPNs SAR (c).

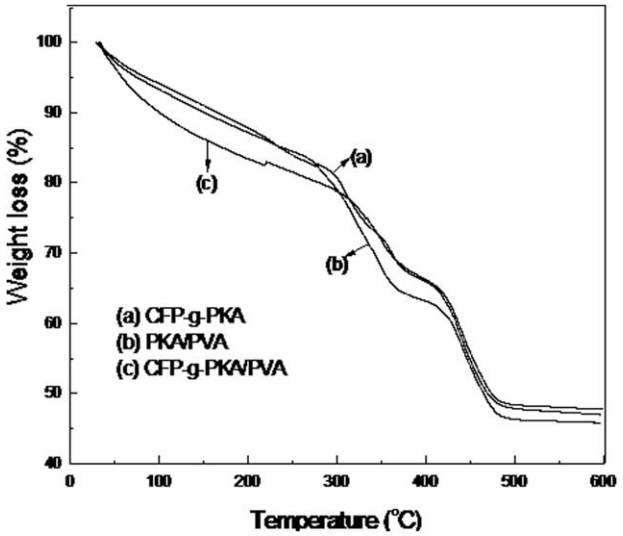

Figure 4. TGA thermogram of CFP-*g*-PKA SAR (a) and PKA/PVA SAR (b) and CFP-*g*-PKA/PVA semi-IPNs SAR (c).

the reaction.[18] Based on the information revealed in Figure 2, it could obtain that grafting polymerization of AA onto CFP and further semi-interpenetrating with PVA occurred during the chemosynthesis, and the resulting product was a composite based on PKA incorporating with CFP and PVA.

SEM Results

In this article, SEM was used to investigate and identify the differences of surface morphology, size, shape and porosity between CFP-*g*-PKA SAR, PKA/PVA SAR, and CFP-*g*-PKA/PVA semi-IPNs SAR [Figure 3(a–c)]. As can be seen, compared with CFP-*g*-PKA/PVA semi-IPNs SAR, the samples of CFP-*g*-PKA SAR and PKA/PVA SAR had comparatively smooth and tight surfaces. However, the undulant, coarse and porous surface of CFP-*g*-PKA/PVA semi-IPNs SAR was ascribed to introduction of CFP and PVA. This porous microstructure increased surface area and was useful for water penetrating into the polymeric network of SAR, resulting in the improvement of water absorbency.[19] The well-connected surface existed in semi-IPNs SAR confirmed the three-dimensional structure and the enhancement of the response rate during the process of swelling.

TGA Results

TGA curves of CFP-g-PKA SAR (a), PKA/PVA SAR (b) and CFP-g-PKA/PVA semi-IPNs SAR (c) were shown in Figure 4. It was observed that with temperature increasing from 33 to 595°C, all of the curves showed a two-step thermogram and the total weight loss were 53.04 54.08 and 50.24%, respectively. The same weight loss occurred between 90–110°C and 387–413°C were suggested to be due to the water evaporation and the thermal decomposition of the carboxyl groups of PKA chain, respectively.[20] The weight loss occurred between 340 and 390°C

Table I. Effects of AA, PVA, Initiator, MBA on Water Absorbency of Semi-IPNs SAR

Various conditions in synthesis		*The water absorbency in distilled water (g/g)*	*The water absorbency in 0.9 wt % NaCl solution(g/g)*	*ΔS.E. (%)*
The weight ratio of	*8 : 1*	*408.4*	*46.12*	*3.3*
AA (g) to CFP (g)	*9 : 1*	*452.8*	*49.44*	*4.0*
	10 : 1	*598.6*	*55.35*	*3.6*
	11 : 1	*635.1*	*57.97*	*3.4*
	12 : 1	*666.2*	*62.26*	*4.2*
	13 : 1	*629.8*	*54.69*	*4.0*
	14 : 1	*604.6*	*51.32*	*4.6*
The weight ratio of	*0*	*279.3*	*30.04*	*3.1*
PVA (g) to CFP (g)	*1 : 1*	*533.0*	*49.86*	*3.2*
	1.5 : 1	*628.7*	*60.55*	*4.3*
	2 : 1	*684.5*	*66.32*	*4.1*
	2.5 : 1	*612.9*	*62.40*	*4.5*
	3 : 1	*548.2*	*52.28*	*4.8*
The weight ratio of	*1*	*479.6*	*44.03*	*3.5*
$K_2S_2O_8$ to AA (%)	*1.5*	*568.2*	*51.96*	*3.2*
	2	*692.5*	*64.23*	*3.7*
	2.5	*616.8*	*53.74*	*4.4*
	3	*529.4*	*48.66*	*4.2*
The weight ratio of	*0.16*	*568.1*	*53.74*	*4.3*
MBA to AA (%)	*0.32*	*714.2*	*70.08*	*3.9*
	0.48	*618.9*	*59.51*	*4.2*
	0.60	*542.6*	*51.79*	*4.6*
	0.72	*495.5*	*50.24*	*4.4*

[Figure 4(a)] was ascribed to the degradation of protein in the graft copolymer. In Figure 4(b), the degradation behavior of PVA possessed two steps, which were the first degradation step (side chain decomposition of PVA) between 280 and 350°C and the second degradation step (main chain decomposition of PVA) between 400 and 470°C.[8] Compared with CFP-*g*-PKA and PKA/PVA SAR, CFP-*g*-PKA/PVA semi-IPNs SAR showed lower total weight loss within the same temperature range. The TGA results implied that CFP-*g*-PKA/PVA semi-IPNs SAR had improved thermal stability. Moreover, it confirmed that the graft copolymerization reaction was taken place among CFP, AA, and PVA.

Effect of Weight Ratios of AA to CFP and PVA to CFP on Water Absorbency of Semi-IPNs SAR

The effects of weight ratios of AA to CFP and PVA to CFP on water absorbency of the CFP-*g*-PKA/PVA semi-IPNs SAR were investigated and shown in Table I (reaction conditions: weight ratios of $K_2S_2O_8$ to AA and MBA to AA, 2 and 0.32%; neutralization degree of AA, 75 mol %; reaction temperature, 50°C; reaction time, 4 h). As the basic skeleton, each protein unit could not be broken and the main reaction of the first step (as depicted in Figure 1) was activation. A large proportion of the reaction function groups, such as —COOH groups in AA, —NH_2, and —OH groups in protein could be grafted in the second step, resulting in the ratio of graft was about 73.3%,[21] and the yield of SAR obtained 80%. The results showed that water absorbency increased continuously with increasing weight ratio of AA to CFP in the range of 8–12, and the water absorbency of semi-IPNs SAR in distilled water and 0.9 wt % NaCl solution increased from 408.38 to 666.2 g g^{-1} and 46.12 to 62.26 g g^{-1}, respectively. This can be explained that CFP contained plenty of non-ionic hydrophilic groups, such as amino, carboxyl and phenolic groups. As the weight ratio of AA to CFP increased, the higher monomer concentration would cause more AA molecules to be grafted onto the backbone of CFP,[22] which enhanced hydrophilicity of SAR and more hydrophilic groups such as —OH, —COO^-, and —COOH were grafted onto the CFP, resulting an increase in water absorbency. However, when the weight ratio of AA to CFP was above 12, water absorption decreased. The reason lied in the fact that when the amount of AA was high, the monomer was superfluous in the reaction system. The network of polymer became closer and the superfluous AA turned to be a homopolymer PKA, which cannot contribute to the water absorbency.[23] So, soluble materials at fixed cross-linking density[24] increased, the expansion of net structure and the movement of free radicals were restricted, which resulted in the drop of water absorbency.

The weight ratio of PVA to CFP played a key role in impacting water absorbency of the semi-IPNs SAR (depicted in Table I). As the weight ratio of PVA to CFP changed in the range of 0 to 2, the water absorbency of SAR in distilled water and 0.9 wt % NaCl solution increased from 279.3 to 684.5 g g^{-1} and 30.04 to 66.32 g g^{-1}, respectively. It could be concluded that with the increase of PVA content, more nonionic hydrophilic groups, such as —OH could react with CFP-*g*-PKA during the polymerization process and improved the polymeric network, so enhanced the water absorption ability. However, when PVA was excessive, the contents of linear polymer in SAR increased, reducing the volume of the network structure. The redundant PVA can not be enwrapped efficiently by SAR and congested in the void or interspace of polymeric network,[25] therefore the osmotic pressure between the polymeric network and external solution decreased,[26] which impeded water pervasion and lead to the decline of water absorbency.

Effect of Initiator Content on Water Absorbency

In the present work, the three initiators, i.e., $K_2S_2O_8$, Na_2SO_3 and $(NH_4)_2Ce(NO_3)_6$ were combined to form a oxidation and reduction system. The best mass ratios between the three initiators were $m(K_2S_2O_8) : m(Na_2SO_3) = 3 : 1$ and $m((NH_4)_2Ce(NO_3)_6) : m(K_2S_2O_8) = 1 : 5$.[27] The effect of the initiator content on the water absorbency of the CFP-g-PKA/PVA semi-IPNs SAR was studied with various contents of initiator, which was referred as the weight percent of $K_2S_2O_8$ to AA (reaction conditions: weight ratios of AA to CFP and PVA to CFP, 12 and 2; weight ratio MBA to AA, 0.32%; neutralization degree of AA, 75 mol %; reaction temperature, 50°C; reaction time, 4 h). It can be observed in Table I that with the increase of initiator content from 1.0 to 2.0 wt %, water absorbency increased and reached the maximum at 2.0 wt %, and then decreased with further initiator content increasing. It was ascribed to the fact that when the dosage of initiator was low, free radicals of protein molecules couldn't be fully produced and the polymerization was tardive, which led to less grafted points and grafted monomer amount. As a result, effective three-dimensional polymer network couldn't be formed, which might result in low water absorbency. With the increase of initiator content, more graft polymerization occurred between AA and CFP, which led to the formation of more stable network structures and contribute to the enhancement of water absorbency. However, when initiator content exceeded 2.0 wt %, the rush out of plethoric free-radicals caused popcorn polymerization and terminating step due to the heat accumulation originated from the too fast polymerization, and the crosslinking density was very high, accompanying by low molecular weight SAR and weak water absorption capacity.[25,28]

Effect of Crosslinker Content on Water Absorbency

In the present work, the weight ratio of MBA to AA had been varied in the range of 0.16–0.72 wt %, and the results (depicted in Table I) of this variation showed that crosslinker content was the most significant influencing factor on the water absorbency (reaction conditions: weight ratios of AA to CFP and PVA to CFP, 12 and 2; weight ratio $K_2S_2O_8$ to AA, 2%; neutralization degree of AA, 75 mol %; reaction temperature, 50°C; reaction time, 4 h).The maximum water absorbency of SAR in distilled water and 0.9 wt % NaCl solution were 714.2 and 70.08 g g^{-1}, respectively, and obtained at 0.32%. A further increase or decrease of MBA content caused the decline of water absorbency. Based on Flory's network theory,[29] it can be inferred that crosslinking density played a major role in modifying the water absorbency of superabsorbents. When the weight ratio of MBA to AA was lower than 0.32 wt %, the crosslinking density was low, which resulted in the decreasing of the gel strength of semi-IPNs SAR. So, the semi-IPNs SAR would become water soluble resin after water absorbed. And the water absorption was low. As the crosslinking density increases, more three-dimensional

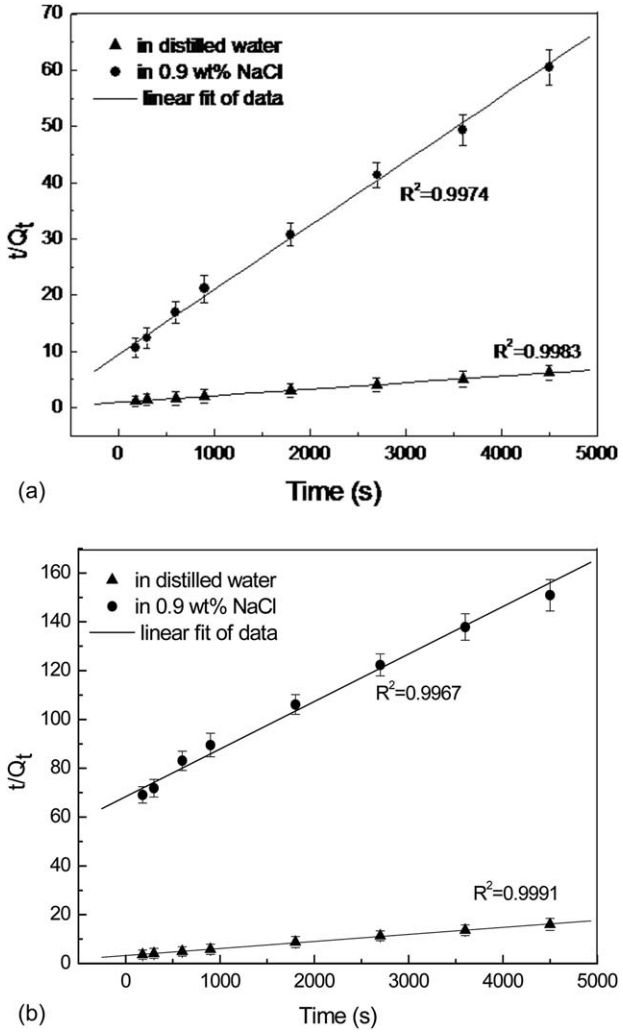

Figure 5. Swelling kinetic curves of CFP-*g*-PKA/PVA semi-IPNs SAR (a) and CFP-*g*-PKA SAR (b) in distilled water and 0.9 wt % NaCl solution.

polymer network with small aperture formed, which would contribute to the water absorbency of semi-IPNs SAR. However, higher MBA content resulted in the generation of more crosslinking points, which caused the formation of additional network and decreased the available free volume within the superabsorbent polymer network.[30,31] Moreover, the elasticity of the polymeric network of the superabsorbent decreased, which was responsible for the decrease of water absorbency.

Swelling Kinetics

The swelling kinetics of CFP-*g*-PKA/PVA semi-IPNs SAR and CFP-*g*-PKA SAR in distilled water and 0.9 wt % NaCl were evaluated by Schott's pseudo second order kinetics model.

$$t/Q_t = 1/K_{is} + (1/Q_\infty)t. \quad (2)$$

where Q_t (g g^{-1}) was the water absorption of SAR at time t; Q_∞ (g g^{-1}) was the theoretical equilibrium swelling capacity; K_{is} was the initial swelling rate constant (g g^{-1} s^{-1}). As can be seen in Figure 5, the plot of t/Q_t versus t gave straight lines and the linear correlation coefficients of the lines were all >0.99. The results indicated that the pseudo second order model can be effectively used to evaluate swelling kinetics of SARs. Q_∞ and K_{is} of SARs can be calculated by the slope and intercept of each fitted straighted line. For CFP-g-PKA/PVA, Q_∞ values were 909.09 and 85.47 g g^{-1}, K_{is} were 0.9313 and 0.103 g g^{-1} s^{-1} in distilled water and 0.9 wt % NaCl solution, respectively. For CFP-g-PKA, Q_∞ values were 341.63 and 34.52 g g^{-1}, K_{is} were 0.3408 and 0.052 g g^{-1} s^{-1} in distilled water and 0.9 wt % NaCl solution, respectively. It can be concluded that the swelling capacity and swelling rate in distilled water were much higher than in 0.9 wt % NaCl solution, and the incorporation of PVA improved the swelling capacity and initial swelling rate of SAR.

Effect of pH on Swelling Kinetics

The swelling behavior of CFP-*g*-PKA/PVA semi-IPNs SAR in various pH value solutions ranged from 2 to 12 was investigated and shown in Figure 6. Because absorbency of SAR was strongly affected by ionic strength, no additional ions (through buffer solution) were added to medium for setting pH.[32] NaOH and HCl solutions were used to adjust solutions with desired basic and acidic pHs.[33] As pH changing in the range of 2–6, the water absorption capability increased continuously. This was attributed to the fact that the carboxylic groups became ionized and the electrostatic repulsion between the molecular chains was predominated which lead to the network more expanding.[34,35] When pH value is too low (such as pH = 2), most of —COO$^-$ groups change into —COOH groups, resulting in the increase of the screening effect of the counterion on the polyanion chains. Meanwhile, HCl solution would ionize more Cl$^-$, which decreased the osmotic pressure difference between external solution and SAR, so water absorbency was much lower.[22] The reason for the swelling loss in the highly basic solutions (pH > 8) was due to the "charge screening effect" of excess Na$^+$ in the swelling media, which shielded the carboxylate and sulfonate anions and prevented effective anion–anion repulsion. Similar swelling-pH dependencies have been reported in the case of other SAR systems.[36] When the pH value was too high, most of —COOH change into —COO$^-$ groups, which resulted in the decrease of repulsion among polymeric chains and consequentially leads to decrease of water absorbency.[22]

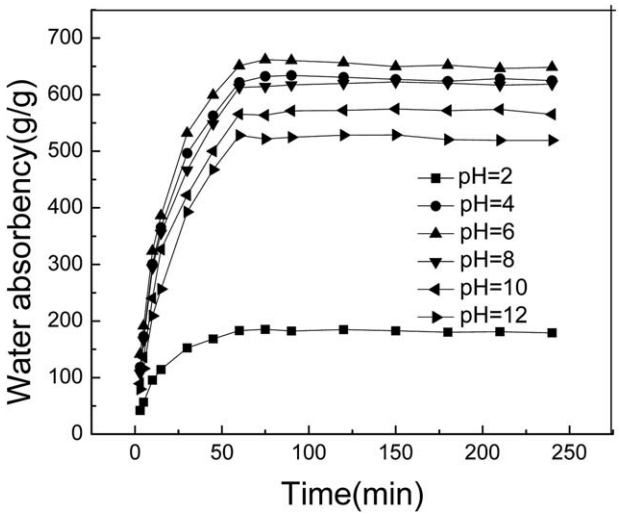

Figure 6. Effect of pH on swelling kinetics of CFP-*g*-PKA/PVA semi-IPNs SAR.

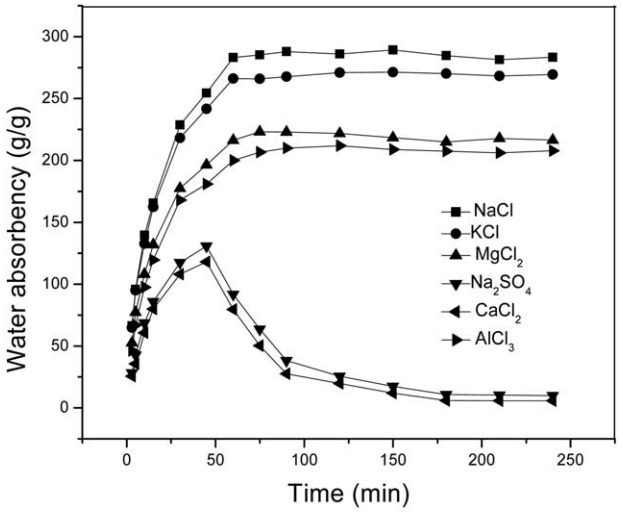

Figure 7. Effect of various salt solutions on swelling kinetics of CFP-*g*-PKA/PVA semi-IPNs SAR.

Effect of Various Saline Solutions on Swelling Kinetics

To better understand the swelling behaviors of SAR in presence of various cations and anions, the chloride salts of Na^+, K^+, Mg^{2+}, Ca^{2+}, Al^{3+} and sodium sulfate with the concentration of 10 mmol L^{-1} were employed as swelling media. The results showed in Figure 7 appreciably demonstrated that comparing with distilled water, the swelling ratio in saline solutions was clearly decreased. As can be seen, the water absorbency in all salt solutions reached swelling equilibrium within 60 min and followed the order of swelling ratio i.e., $Na^+ > K^+ > Mg^{2+} > Ca^{2+} > Al^{3+}$ (cations) and $Cl^- > SO_4^{2-}$ (anions). This fact was mainly caused by the size of the ions, with increase in the size, the ions were much difficult to penetrate into the semi-interpenetrated networks of the SAR. The absorbency of the CFP-*g*-PKA/PVA semi-IPNs SAR in salt solutions was monovalent > bivalent cations > trivalent cations. It may be additionally caused by complexing ability arising from the coordination of the trivalent or bivalent cations with superabsorbent groups.[33] The complexing ability of carboxylate groups on the SAR could induce the formation of intramolecular and intermolecular complexes with the bivalent cations, resulting in the reduction of water penetrated into the networks of SAR. So the swelling capacity and swelling rate of semi-IPNs SAR decreased with the increase of the ion size presented in the swelling medium.[37]

The swelling behavior differences between the monovalent anion (Cl^-) and the divalent anion (SO_4^{2-}) were due to the different ionic strengths, which produced a different osmotic pressure to prevent water from being absorbed.[38] Another possible reason in lowering the swelling capacity of the semi-IPNs SAR in $MgCl_2$, $CaCl_2$ and $AlCl_3$ solutions was that the bivalent magnesium or calcium ions and trivalent aluminum ions increased the crosslinking density because of interaction of these metal cations with carboxylate ions leading to "ionic crosslinking."[37] However, swelling behavior in $CaCl_2$ and $AlCl_3$ solutions was quite distinct from others. With the increase of immersing time the water absorbency of SAR increased during the first 60 min, and then decreased close to 10.00 and 5.85 g g^{-1}, respectively. This phenomenon was actually known as the overshooting effect, which can be interpreted as the consequence of a swelling–deswelling process. In $CaCl_2$ and $AlCl_3$ solutions, the spread of polymer network was attribute to the water penetration, meanwhile, a much more crosslink degree was formed during the interaction between Ca^{2+} ions, Al^{3+} ions and carboxyl groups of SAR, which led to a lower swelling.

CONCLUSIONS

In this study, a novel eco-friendly CFP-*g*-PKA/PVA semi-IPNs SAR was successfully prepared by graft copolymerization of AA onto CFP in the presence of PVA. FTIR measurements testified the composition of the semi-IPNs SAR, and the SEM images revealed that the structure of SAR changed with the reaction of CFP and PVA. The TGA technique was employed to successfully characterize the weight loss and grafting information of SAR. The results of single factor analysis showed that the optimum condition was that the weight ratio between CFP, AA, and PVA was m(CFP) : m(AA) : m(PVA) = 1 : 12 : 2. The maximum water absorbency of semi-IPNs SAR in distilled water and 0.9 wt % NaCl solutions were 714.22 and 70.08 g g^{-1}, respectively. The Schott's pseudo second order kinetics model presented high coefficient of determination in distilled water and 0.9 wt % NaCl solution, which provided evidence for future study. Overall, the study demonstrated that, the SAR exhibited pH-sensitive behavior and the water absorbency reached maximum at pH = 6. Swelling capacity for SAR in salt solutions with the same concentration was in order $NaCl > KCl > MgCl_2 > Na_2SO_4 > CaCl_2 > AlCl_3$. The superior performances of CFP-*g*-PKA/PVA semi-IPNs SAR could promote their potential applications in agriculture and horticulture fields.

ACKNOWLEDGMENTS

The authors are grateful for financial support from National Natural Science Foundation of China (21007034) and Natural Science Foundation of Shandong Province (ZR2010EQ031).

REFERENCES

1. Zhang, J.; Wang, A. *React. Funct. Polym.* **2007**, *67*, 37.
2. Ding, X. X.; Zheng, Z. X.; Xue, C. S.; Xi, Z. R.; John, F. K. *Carbohydr. Polym.* **2007**, *68*, 416.
3. Sperling, L. H. *Polymer* **1984**, *18*, 3593.
4. Čulin, J.; Šmit, I.; Andreis, M.; Veksli, Z.; Anžlovar, A.; Žigon, M. *Polymer* **2005**, *46*, 89.
5. Chen, J.; Liu, M. Z.; Liu, H. L.; Ma, L. W.; Gao, C. M.; Zhu, S. Y.; Zhang, S. P. *Chem. Eng. J.* **2010**, *159*, 247.
6. Chang, C. Y.; Duan, B.; Cai, J.; Zhang, L. N. *Eur. Polym. J.* **2010**, *46*, 92.
7. Lawal, O. S.; Storz, J.; Storz, H.; Lohmann, D.; Lechner, D.; Kulicke, W. M. *Eur. Polym. J.* **2009**, *45*, 3399.
8. Dragan, E. S.; Lazar, M. M.; Dinu, M. V.; Doroftei, F. *Chem. Eng. J.* **2012**, *204*, 98.
9. Tonkova, E. V.; Gousterova, A.; Neshev, G. *Int. Biodeter. Biodegrad.* **2009**, *63*, 1008.
10. Böckle, B.; Galunsky, B.; Müller, R. *Appl. Environ. Microbiol.* **1995**, *61*, 3705.

11. Odetallah, N. H.; Wang, J. J.; Garlich, J. D.; Shih, J. C. H. *Poultry Sci.* **2003**, *82*, 664.
12. Choi, J. M.; Nelson, P. V. *J. Am. Soc. Horticultural Sci.* **1996**, *12*, 634.
13. Coward-Kelly, G.; Chang, V. S.; Agbogbo, F. K.; Holtzapple, M. T. *Bioresource Technol.* **2006**, *97*, 1337.
14. Sharma, R.; Gupta, R. *Bioresource Technol.* **2012**, *120*, 314.
15. Banerjeea, S.; Siddiqui, L.; Bhattacharya, S. S.; Kaity, S.; Ghosh, A.; Chattopadhyay, P. P.; Singh, L. *Int. J. Biol. Macromol.* **2012**, *50*, 198.
16. Luke, R. B.; Maria, B. R.; Jillian, R. R.; Tamer, A. A.; Daniel, E.; Catherine, L. W.; Giuseppe, O.; Roy, R. H.; Mark, E. V. D. *Biomaterials* **2013**, *34*, 2632.
17. Guo, J.; Jin, Y. C.; Yang, X. Q.; Yu, S. J.; Yin, S. W.; Qi, J. R. *Food Hydrocolloids* **2013**, *31*, 220.
18. Li, A.; Zhang, J. P.; Wang, A. Q. *Bioresource Technol.* **2007**, *98*, 327.
19. Liang, R.; Yuan, H. B.; Xi, G. X.; Zhou, Q. X. *Carbohydr. Polym.* **2009**, *77*, 181.
20. Chen, Y.; Tan, H. M. *Carbohydr. Res.* **2006**, *341*, 887.
21. Singha, A. S.; Rana, R. K. *Carbohydr. Polym.* **2012**, *87*, 500.
22. Liu, J. H.; Wang, Q.; Wang, A. Q. *Carbohydr. Polym.* **2007**, *70*, 166.
23. Hua, S. B.; Wang, A. Q. *Carbohydr. Polym.* **2009**, *75*, 79.
24. Finkenstadt, V. L.; Willett, J. L. *Macromol. Chem. Phys.* **2005**, *206*, 1648.
25. Zhong, K.; Zheng, X. L.; Mao, X. Y.; Lin, Z. T.; Jiang, G. B. *Carbohydr. Polym.* **2012**, *90*, 820.
26. Liu, Z.; Miao, Y.; Wang, Z. *Carbohydr. Polym.* **2009**, *77*, 131.
27. Guo, Y.; Li, X.; Li, C. *Fine Chem.* **2006**, *23*, 31.
28. Allcock, H. R.; Frederick, W. L. Contemporary Polymer Chemistry; Prentice Hall: Englewood Cliffs, NJ, **1981**.
29. Flory, P. J. Principles of Polymer Chemistry; Cornell 563 University Press: New York, **1953**.
30. Li, A.; Wang, A. Q.; Chen, J. M. *J. Appl. Polym. Sci.* **2004**, *92*, 1596.
31. Chen, J. W.; Zhao, Y. M. *J. Appl. Polym. Sci.* **2000**, *74*, 119.
32. Zheng, Y.; Liu, Y.; Wang, A. Q. *Chem. Eng. J.* **2011**, *171*, 1201.
33. Bao, Y.; Ma, J. Z.; Li, N. *Carbohydr. Polym.* **2011**, *84*, 76.
34. Li, X.; Xu, S. M.; Wang, J. D.; Chen, X. Z.; Feng, S. *Carbohydr. Polym.* **2009**, *75*, 688.
35. Chen, Y.; Liu, Y. F.; Tang, H. L.; Tan, H. M. *Carbohydr. Polym.* **2010**, *81*, 365.
36. Lanthong, P.; Nuisin, R.; Kiatkamjornwong, S. *Carbohydr. Polym.* **2006**, *66*, 229.
37. Keshava Murthy, P. S.; Murali Mohan, Y.; Sreeramulu, J.; Mohana Raju, K. *React. Funct. Polym.* **2006**, *66*, 1482.
38. Zheng, Y.; Li, P.; Zhang, J. P.; Wang, A. Q. *Eur. Polym. J.* **2007**, *43*, 1691.